Fast Photovoltaic Array Reconfiguration for Partial Solar Powered Vehicles

Jaemin Kim[1] , Yanzhi Wang[2] , Massoud Pedram[2] , and Naehyuck Chang[1]
[1]Seoul National University, Seoul, Korea
[2]University of Southern California, Los Angeles, CA, USA
[1]{jmkim,naehyuck}@elpl.snu.ac.kr, [2]{yanzhiwa,pedram}@usc.edu

ABSTRACT

This paper demonstrates that a partially solar powered EV can significantly save battery energy during cruising using innovative fast photovoltaic array (PV) reconfiguration. Use of all the vehicle surface areas, such as the hood, rooftop, door panels, quarter panels, etc., makes it possible to install more PV modules, but it also results in severe performance degradation due to inherent partial shading. This paper introduces fast online PV array reconfiguration and customization of the PV array installation according to the driving pattern and overcomes the partial shading phenomenon. We implement a high-speed, high-voltage PV reconfiguration switch network with IGBTs (insulated-gate bipolar transistors) and a controller. We derive the optimal reconfiguration period based on the solar irradiance/driving profiles using adaptive learning method, where the on/off delay of IGBT, CAN (control area network) delay, computation overhead, and energy overhead are taken into account. Experimental results show 25% more power generation from the PV array. This paper also introduces two important design-time optimization problems to achieve trade-off between performance and overhead. We derive the optimal PV reconfiguration granularity and partial PV array mounting by the car owner's driving pattern, which results in more than 20% PV cell cost reduction.

1. INTRODUCTION

Photovoltaic (PV) cells are clean, light weight, quiet, and durable, and thus may be an ideal power source for electric vehicles (EV) [1, 2, 3]. Unfortunately, PV power alone seems simply not sufficient to operate a full EV [2]. The highest solar irradiance in a day (at noon time) is at around 1000 W/m^2, and a 30% efficiency PV module with 1 m^2 area generates 300 W peak power. Typical horizontal panel areas such as the rooftop, hood and trunk of a passenger vehicle are around 4 - 5 m^2. On the other hand, modern electric vehicles (EV) aim at similar or even higher driving performance compared with conventional internal combustion engine vehicles as well as fuel economy and zero emission. Their traction motor power rating is commonly over 100 kW [4]. However, most vehicle horsepower is mainly for acceleration and uphill driving, whereas vehicles use a small fraction during cruising (e.g., less than 10 kW during city driving.) Hence, although full PV powered driving is not practical in normal passenger cars and driving conditions, partial PV power driving is certainly beneficial [2]. The PV cells can also charge the EV battery when the EV is parked, thereby mitigating the charging requirement from the grid.

PV power has lots of advantages because a large portion of electricity that charges EV is generated from fossil fuel. The current PV powered EV is equipped with PV cells on the vehicle panels that has the smallest solar incidence angle such as the hood and the rooftop. It is certainly meaningful to enlarge the onboard PV cell array using more vehicle surface area such as door panels and quarter panels.

The *string charger architecture* [5], where a single power converter is connected to both ends of the whole PV cell array (including PV modules on the hood, rooftop, door panels, quarter panels, etc.), is a practical method considering the cost. In addition, EVs are equipped with high-voltage batteries to achieve low IR loss, and thus the use of *micro-charger architecture* (i.e., multiple power converters, each connecting to a PV module mounted on the hood, the rooftop, door panels, quarter panels, etc.) is not only expensive but also inefficient to step up the PV voltage [5]. However, PV cells on the door and quarter panels may not help increase or may even decrease the PV power output because the solar irradiance on these panels may be largely different from that on the hood and the rooftop. Moreover, the solar irradiance profiles on the driver-side quarter and door panels and the passenger-side panels are virtually opposite by the driving direction and time of the day.

Combined usage of the PV modules on the rooftop, hood, trunk, quarter, and door panels are challenging in maintaining high performance in a string charger architecture. This paper introduces a fast PV cell array reconfiguration for the partial solar powered EV. We borrow the dynamic PV module reconfiguration architecture from previous work [6, 7, 8]. However, the solar irradiance levels are rapidly changing in the case of PV modules on the vehicle due to nearby shading and direction changes. We implement a high-speed, high-voltage PV reconfiguration switch network with IGBTs (insulated-gate bipolar transistors) and a controller. We derive the optimal reconfiguration period considering the on/off delay of IGBT, CAN (control-area network) delay, computation overhead, and energy overhead. We carefully decide the reconfiguration policy based on the solar irradiance/driving profiles using adaptive learning [9].

We solve a design-time optimization problem of deriving the optimal granularity of PV reconfiguration to achieve a desirable trade-off of performance and reconfiguration complexity/overhead. This paper also introduces *partial PV installation*. As PV modules are still costly, installation of a low-efficiency PV module is a waste. For example, the driver-side quarter and door panels do not have

ISLPED '14 La Jolla, CA USA

http://dx.doi.org/10.1145/2627369.2627623.

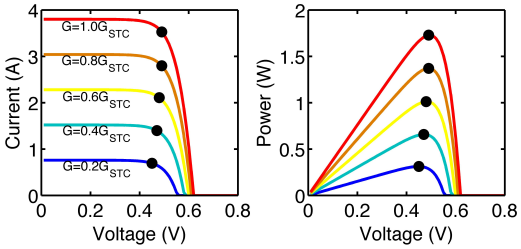

Figure 1: I-V and P-V characteristics of a PV cell.

meaningful solar irradiance when a driver commutes to the northbound in the morning and the southbound in the afternoon. We implement an onboard PV irradiance monitoring sensor network and collect various irradiance profiles by the driving location and time, and then we customize the PV module installation according to the driving pattern.

We evaluate the proposed fast dynamic PV reconfiguration technique based on the actual implementation of reconfiguration network and controller. Experiments show that the fast dynamic PV array reconfiguration increases 423.0 W power from the baseline. The customized PV installation reduces 22.3 % PV cell cost showing only 5.6 % reduction of power generation output.

2. COMPONENT AND SYSTEM MODELS

2.1 PV Cell Modeling and Characterization

Every PV module/array is comprised of multiple PV cells. Figure 1 illustrates the PV cell I-V and P-V characteristics under different solar irradiance levels G's, where G_{STC} stands for the irradiance (1000 W/m^2) at standard test condition. One can observe that the PV cell exhibits a nonlinear output current and voltage relationship. There is an MPP under any solar irradiance level, where the output power of the PV cell is maximized. MPPs are labeled by black dots in Figure 1.

Power converters or chargers are necessary in PV systems for controlling the output voltage and current of PV modules [10]. The maximum power point tracking (MPPT) and maximum power transfer tracking (MPTT) techniques have been proposed to maximize the output power of PV systems under changing solar irradiance [10, 11, 12].

2.2 String Charger Architecture

The system diagram of the vehicular PV system is illustrated in Figure 2 based on the string charger architecture. The whole PV cell array may be comprised of multiple PV modules mounted on the hood, rooftop, door panels, quarter panels, etc., of the vehicle. Different PV modules have different areas and thus different numbers of PV cells. We use a charger between the whole PV cell array and the vehicular battery pack in order to properly regulate the operating point of the PV array. A buck-boost charger power model is proposed in [13]. In general, the charger efficiency is maximized when (i) its input and output voltages are close to each other, and (ii) the output current is within a certain range.

3. PV ARRAY RECONFIGURATION

3.1 Reconfiguration Structure

A conventional PV array consists of n series-connected PV groups, whereby each PV group has exactly m parallel-connected PV cells. Solar irradiance levels received by different PV cells in the array

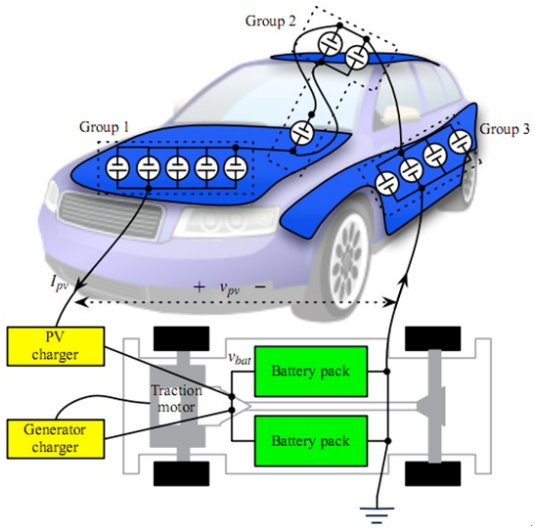

Figure 2: System diagram of a PV system on electric vehicles.

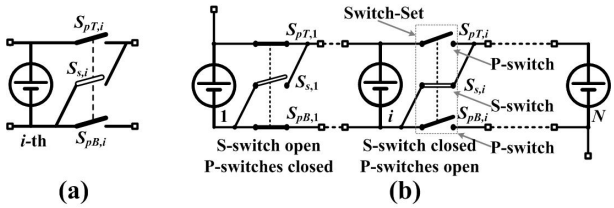

Figure 3: The structure of a reconfigurable PV array.

may be different, and such a phenomenon is known as the *partial shading effect*, which can be resulted from moving vehicles, nearby buildings and obstacles [6]. The PV array mounted on vehicles experiences more significant partial shading effect because changing directions will result in changes of solar irradiance levels at different sides of the vehicles. Partial shading not only reduces the maximum output power of the shaded PV cells, but also makes the lighted or less-shaded PV cells that are connected in series with the shaded ones deviate from their MPPs, thereby degrading the output power of the PV array.

Reference work [6, 7] suggested dynamic PV array reconfiguration to combat partial shading. The proposed reconfiguration technique can make both the shaded and lighted PV cells work at or close to their MPPs simultaneously, thereby improving the PV system output power. Figure 3 shows the structure of a reconfigurable PV array [6] with N PV cells. Please note that for the vehicular PV array, the reconfiguration structure connects all the PV cells from all PV modules mounted on the hood, rooftop, door panels, quarter panels, etc., of the vehicle[1].

As shown in Figure 3, each of the PV cells (except for the N-th PV cell) in the reconfigurable structure is integrated with three solid-state switches: a top parallel switch $S_{pT,i}$, a bottom parallel switch $S_{pB,i}$, and a series switch $S_{S,i}$. PV array reconfiguration can be conducted by controlling the ON/OFF states of the programmable switches. The two parallel switches of a PV cell are always in the same state, and the series switch of a PV cell must be in the opposite state of its parallel switches. The parallel switches connect PV cells in parallel to form a *PV group*, and the series switches connect PV groups in series. In general, a reconfigurable PV array with N PV cells can have a arbitrary number (less than or

[1]This requires negligible additional overhead because only two connection wires are required to connect all the PV modules as shown in Figure 3.

equal to N) of PV groups, each with arbitrary number of PV cells with consecutive IDs. Now we provide the formal definition of the configuration of a reconfigurable PV array. Consider a reconfigurable PV array comprised of N PV cells, it can have an arbitrary number (less than or equal to N) of PV groups. The number r_j(>0) of parallel-connected PV cells in the j-th PV group should satisfy:

$$\sum_{j=1}^{g} r_j = N, \tag{1}$$

where g is the number of PV groups. This configuration can be viewed as a partitioning of the PV cell index set $\mathbf{A} = \{1, 2, 3, ...N\}$, where the elements in $\mathbf{A}$ denote the indices of PV cells in the array. This partitioning is denoted by subsets $\mathbf{B}_1$, $\mathbf{B}_2$, ..., and $\mathbf{B}_g$ of $\mathbf{A}$, which correspond to the g PV groups comprised of r_1, r_2, ..., and r_g PV cells, respectively. The subsets $\mathbf{B}_1$, $\mathbf{B}_2$, ..., and $\mathbf{B}_g$ satisfy

$$\cup_{j=1}^{g} \mathbf{B}_j = \mathbf{A} \tag{2}$$

and

$$\mathbf{B}_j \cap \mathbf{B}_k = \emptyset, \quad \forall j, k \in \{1, 2, ..., g\}, \quad j \neq k \tag{3}$$

The indices of PV cells in group j must be smaller than the indices of PV cells in group k for any $1 \leq j < k \leq g$ due to the structural characteristics of the reconfigurable PV array, i.e., $i_1 < i_2$ for $\forall i_1 \in \mathbf{B}_j$ and $\forall i_2 \in \mathbf{B}_k$ satisfying $1 \leq j < k \leq g$. A partitioning satisfying the above properties is called an *alphabetical partitioning*.

3.2 Reconfiguration Algorithm

Let G_{hood}, G_{roof}, G_{trunk}, G_{left} and G_{right} denote the solar irradiance levels on PV cells mounted on the hood, rooftop, trunk, left side and right side, respectively, of the vehicle. We measure these solar irradiance profiles using solar sensor network to be discussed later. Based on these irradiance levels, we derive the optimal configuration of the PV panel based on the polynomial-time reconfiguration algorithm provided in [6], which is comprised of an outer loop to find the optimal number of groups in the PV array and a kernel algorithm to determine the optimal configuration based on the number of groups. Under rapidly-changing irradiance levels on each side of the vehicle during driving, it is not possible to perform optimal reconfiguration as long as some irradiance level changes due to the timing and energy overhead associated with reconfiguration. Thus, we need to determine the optimal reconfiguration policy (and period) for the vehicular PV array based on a thorough overhead analysis.

4. SOLAR SENSOR NETWORK AND IRRADIANCE PROFILE ACQUIREMENT

We build a Zigbee-based solar sensor nodes network and a logger program to acquire real solar irradiance profile on each side of vehicles during driving. The actual implementation of a sensor node in the network is provided in Figure 4. Zigbee is a wireless network protocol to create personal area networks, which is commonly used for applications requiring low power, low data rate, and long battery life. The physical transceiving range of Zigbee protocol is up to 120 meters, however, we disable the boost mode to reduce power consumption. We use dual AAA-size batteries to supply power for each node without DC-DC converter to minimize power loss. A Zigbee transceiver module and an ambient sensor can operate by 2.4 V to 3.3 V supply voltage level, which has a enough operation margin for dual alkaline batteries. The lifetime of dual AAA batteries is more than 12 hours, which is enough for recording solar

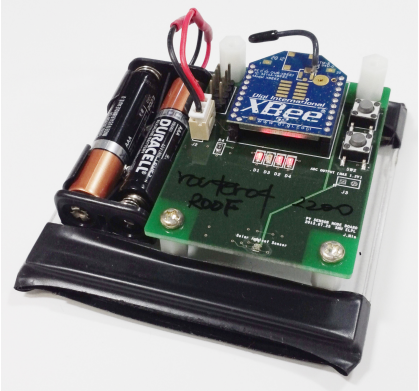

Figure 4: Zigbee-based solar sensor node to measure the solar irradiance.

Table 1: Recorded Driving Profiles.

Location	Start time	End time	Distance
Incheon Airport	12:35	12:43	5.2km
Ontario to Riverside	08:32	08:57	27km
West LA to Indio	12:53	19:50	261.8km
West LA to Carson	14:47	16:31	44.7km
Riverside	14:15	14:36	3.1km
West LA to Riverside	09:58	11:21	112.3km

irradiance profile of one day driving. The Zigbee module automatically reads value from the ambient sensor with its internal ADC and sends it to a receiving node every 50 ms with 250 kbits/s data transmission speed. A specially designed logger program collects irradiance sensor data from the receiving node with vehicle speed and location information from GPS including latitude, longitude, altitude and time. We install magnets to each corner of a sensor node so that the sensor nodes can stick to vehicle easily and firmly. The purpose of this sensor node is to (i) easily attach to any vehicle in a very short amount of time, and (ii) so that we can test various vehicles and locations and collect benchmark solar irradiance profiles.

We attached five sensor nodes at hood, roof, trunk, left side and right side of a vehicle to measure benchmark profiles of G_{hood}, G_{roof}, G_{trunk}, G_{left} and G_{right}, respectively. Finally we drive a vehicle along six paths to collect real benchmark vehicle drive profiles: Seoul to Incheon airport, Ontario to Riverside, west Los Angeles to Indio, west Los Angeles to Carson, Riverside, and west Los Angeles to Riverside. Details are shown in Table 1.

5. RECONFIGURATION HARDWARE DESIGN AND OPTIMIZATION

5.1 PV Reconfiguration Hardware Design

In the PV reconfiguration structure proposed in [6, 8], each switch consists of one MOSFET gate driver and one pair of N-type MOSFETs. However, the reconfigurable PV module array on moving vehicles has different requirements than those in [6, 8]. First, the reconfiguration speed should be highly fast. For example, if there is a shade by an approaching four-meter-long vehicle in the opposite side and the speeds of both vehicles are 80 km/hour, the shade exists for a maximum of 180 ms. Moreover, rapid direction changes of vehicles will result in fast changing in solar irradiance levels at each side of the vehicles. Hence, fast reconfiguration within a few milliseconds reconfiguration time is required to fully exploit the potential benefits of the dynamic reconfiguration capability during ve-

hicle driving. Second, high-voltage or high-current gate control is required for vehicular PV array reconfigurations. We implement an IGBT(insulated-gate bipolar transistor)-based reconfiguration network to meet both requirements.

We carefully select commercial IGBTs and gate drivers for switches in the reconfiguration network. The selected IGBT IXXK200N65B4 can handle voltage and current ratings of 650 V and 370 A, respectively, which is enough rating for vehicular PV arrays. We select gate driver MC33153 that has a short propagation delay of few hundreds nanoseconds to control the IGBTs. We use photo-coupler isolation between the high-voltage IGBT side and the controller logic side to prevent from damage due to power surge. We connect IGBT with 65V/5A rating power supply and apply square-wave input voltage on the gate driver to observe the step response of IGBT. The response waveform of output voltage is not distorted until the input frequency reaches tens of kHz. This shows the stability of the IGBT and gate driver selections.

Then we implement a communication system based on the controller area network, as known as CAN. The CAN standard is established specially for vehicles, which require high stability. The CAN network topology is also a bus structure so that we can easily attach sensor nodes to the communication network. We carefully select ADM3053 as an isolated CAN physical layer transceiver with LM3S2965 as the control processor, which supports hardware layers of CAN communications. 1 Mbps communication speed in transmission will make the transmission delay below 1 ms.

5.2 Overhead Analysis

In order to derive the optimal reconfiguration control policy, we need a thorough analysis of both timing overhead and energy overhead during PV array reconfiguration. During PV array reconfiguration, the following processes are required: sensing the irradiance levels, transmitting the irradiance data from sensors to the central controller, computing the optimal configuration, changing the ON/OFF states of IGBTs, and performing MPPT control after reconfiguration. Hence, the timing overhead of PV array reconfiguration is comprised of the following components:

1. *Sensing delay:* With current sensor network setup, each sensor node senses and converts the solar irradiance value in every 50 ms, which is the sensing period. The sensing delay is less than 10 μs based on the sensor ADC setup.

2. *Network delay:* The transmission delay is no more than 1 ms in the sensor network using CAN transmission protocol.

3. *Computation overhead:* The reconfiguration control algorithm is a polynomial-time optimal algorithm [6]. For a moderate-scale PV array with 60 PV cells, it takes only 3 - 4 ms to calculate the optimal configuration on a 3.0 GHz desktop computer and should take less than 10 ms on a typical ARM-based embedded processor (as the reconfiguration controller) [14].

4. *Reconfiguration delay:* Our experiments show that the gate driver and IGBT can reconfigure within 10 μs with only a little distortion of waveform. so 1 ms will be a safe (conservative) reconfiguration delay.

5. *MPPT control overhead:* The delay of a perturb & observe (P&O)-based MPPT control is typically less than 2.5 ms.

The total timing overhead is the sum of the above-mentioned delay components, and we use 15 ms in our experiments to derive the optimal reconfiguration period. The minimum reconfiguration period is 50 ms which is limited by the sensing frequency. For the energy overhead, the vehicular PV system will have zero output power during reconfiguration (i.e., changing the ON/OFF states of IGBTs) and have sub-optimal output power during P&O-based MPPT control. We use a conservative estimate that the output power will be zero also during the MPPT control period.

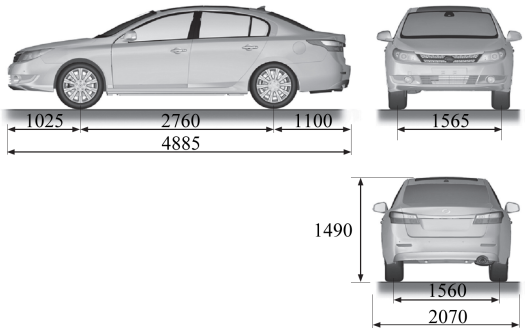

Figure 5: SM5 offical dimension from vehicle manual

5.3 Reconfiguration Period Optimization

Under rapid-changing irradiance levels on each side of the vehicle during driving, it is not possible to perform optimal reconfiguration as long as some irradiance level changes due to the timing and energy overhead associated with reconfiguration. Thus, we need to determine the optimal reconfiguration period (and policy) for the vehicular PV array based on the overhead analysis in the previous subsection. A larger reconfiguration period may not be able to capture the fast changes in solar irradiance levels. On the other hand, a smaller reconfiguration period will induce higher timing overhead and energy overhead, and may eventually degrade the PV system performance.

We use the adaptive learning method to derive the optimal reconfiguration period in an online manner [9]. We maintain multiple candidate reconfiguration period values, and choose one value with the currently highest performance at the beginning of each evaluation period (say, 10 minutes.) At the end of this evaluation period, we evaluate all the reconfiguration period values and update their performance using an exponential weighting function [15], and then choose the reconfiguration period value with the highest updated performance level.

5.4 Experimental Results

In this section, we compare the performance between the proposed reconfigurable vehicular PV system with two baseline systems. The proposed system installs reconfigurable PV array on the rooftop, hood, trunk, and left and right door panels. This should be the largest area for potential solar energy harvesting. We consider two baseline setups. Baseline B1 installs solar modules only on the rooftop, hood, and trunk panels without reconfiguration. Baseline B2 installs solar modules on the rooftop, hood, trunk, quarter, and door panels without reconfiguration. We measure a mid-size family sedan Renault-Samsung NEW-SM5 car and observe the following area parameters: hood (bonnet): 1.6 m^2 (1.024 m by 1.565 m), left door, right door: 1.7 m^2 for each (0.616 m by 2.760 m), roof: 1.99 m^2 (1.274 m by 1.565 m), trunk: 0.63 m^2 (0.400 m by 1.565 m). Note: All parameter values are measured on a real car, which are slightly smaller than official dimension in Figure 5. In this section, we assume fixed-size PV cells with 0.15 m^2 area, 20 V MPP voltage, and 2.25 A MPP current at $G = 1000$ W/m^2. We assume 200 V terminal voltage of the vehicle battery pack. We consider a realistic solar charger model with efficiency variations [13].

Table 2: Performance comparison between the proposed reconfigurable PV system with baseline PV systems on the six benchmark profiles.

Benchmark	Proposed	B1	B2
Incheon Airport	1048 W	887.8 W	730.5 W
Ontario to Riverside	518.5 W	288.4 W	343.2 W
West LA to Indio	836.2 W	715.5 W	569.7 W
West LA to Carson	785.7 W	607.2 W	514.1 W
Riverside	1028 W	706.4 W	616.1 W
West LA to Riverside	472.8 W	49.8 W	163.0 W

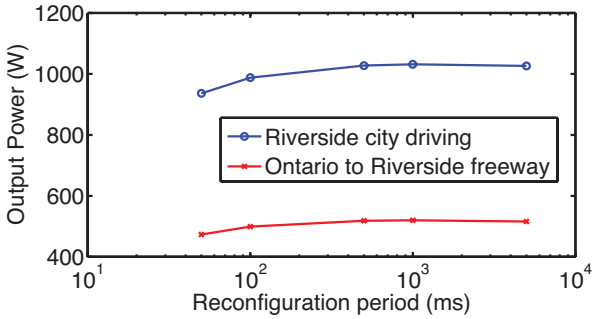

Figure 7: Performance (average output power) of the proposed reconfigurable PV system with different reconfiguration period values on two benchmark profiles.

We first consider a fixed reconfiguration period of 0.5 s, and compare the performance, i.e., the average output power, between the proposed and baseline setups on the six benchmark solar irradiance profiles. Comparison results are illustrated in Table 2. We can observe that the proposed system significantly outperforms baseline setups by a maximum of 423.0 W improvement in average output power. Comparing between two baseline systems, we observe that B1 even often outperforms B2 because the solar irradiances on the left side and right side of the vehicle are often changing and have smaller magnitude compared with the rooftop, which degrades the output power of the PV system. Moreover, we plot the PV array output power versus time of the proposed system and two baseline systems in Figure 6. We can observe that the proposed system consistently outperforms the two baseline systems over the whole time range.

Furthermore, we consider the optimization of reconfiguration period as described in Section 5.3. Figure 7 shows the average output power of the proposed reconfigurable PV system with different reconfiguration period values on two benchmark profiles "Ontario to Riverside" and "Riverside". Please note that 50 ms is the lowest possible reconfiguration period because it is the sensing period. Our experiments show that the optimal reconfiguration periods for the six benchmark profiles are around 0.5 s - 1 s in general, in order to achieve a trade-off between lower timing/energy overhead and fast reconfiguration capabilities.

6. DESIGN-TIME OPTIMIZATION OF THE VEHICULAR PV ARRAY

In this section, we discuss the design-time optimization of the vehicular PV array, including (i) deriving the optimal granularity of PV array reconfiguration, i.e., optimizing the size of a PV cell, and (ii) partial PV array installation. These optimizations are performed statically in the design time, and cannot be altered after installation.

Table 3: Performance comparison of the reconfigurable PV system with different PV cell sizes on the six benchmark profiles.

Profile	0.1 m^2	0.15 m^2	0.25 m^2	0.5 m^2
Incheon Airport	1077W	1048W	1016W	967.5W
Ontario to Riverside	537.9W	518.5W	495.3W	476.1W
West LA to Indio	865.0W	836.2W	799.3W	778.9W
West LA to Carson	809.8W	785.7W	747.5W	726.5W
Riverside	1058W	1028W	993.5W	966.1W
West LA to Riverside	495.6W	472.8W	446.9W	392.3W

6.1 Optimization of PV Cell Size

The PV cell is the basic unit in the reconfiguration technique, and its size is essentially trade-off between the lower additional capital cost and reconfiguration complexity, and performance enhancement. Basically, a larger PV cell size reduces the cost of the reconfigurable PV array architecture since fewer switches are required for reconfiguration and also reduces the computation overhead for the optimal array configuration. A smaller PV cell, on the other hand, achieves better flexibility and thus higher performance against partial shading.

The PV cell size optimization is performed at the system design stage. We aim to find the optimal PV cell size with a capital cost limit to achieve a desirable trade-off between the lower PV system capital cost and reconfiguration overhead, and enhanced performance against partial shading. In the outer loop of algorithm, we use binary search to find the most desirable PV cell size subject to the capital cost constraint. For each given PV cell size inside the loop, we evaluate the PV system performance using the six solar irradiance benchmarks using the corresponding optimal reconfiguration policy. The timing overhead and energy overhead are taken into account in this evaluation procedure.

We set the PV cell lower limit by 0.1m^2 and compare the performance of reconfigurable PV array with different PV cell sizes on the six solar irradiance profiles. We adopt a fixed reconfiguration period of 0.5 s. Table 3 shows the comparison results including four possible PV cell sizes: 0.1 m^2, 0.15 m^2, 0.25 m^2, and 0.5 m^2. We observe that a finer grained PV cell will result in higher average output power (at most 26.3% higher average output power when comparing between the 0.1 m^2 case and 0.5 m^2 case) due to the higher flexibility in reconfiguration. We would like to point out that the timing and energy overhead of all these testing cases are within the estimates provided in Section 5.2.

6.2 Partial PV Array Installation

In this section, we introduce *partial PV array installation*. As PV modules are still costly, installation of a low-efficiency PV module is a waste. For example, the driver-side quarter and door panels do not have meaningful solar irradiance when a driver commutes to the northbound in the morning and the southbound in the afternoon. Based on the PV irradiance profiles collected using the solar sensor network, we propose to customize the PV module installation according to different driving patterns.

More specifically, we consider the following partial solar array installation with reconfiguration: the rooftop, hood and trunk are equipped with PV cells, and either the left side or right side of the vehicle is equipped with PV cells. We compare the performance (output power) of these two customized PV array installation cases with the optimal reconfigurable vehicular PV system. We assume fixed-size PV cells of 0.15 m^2 and adopt a fixed reconfiguration period of 0.5 s. Table 4 shows the comparison results. We can observe that for some benchmark profiles such as "Ontario to River-

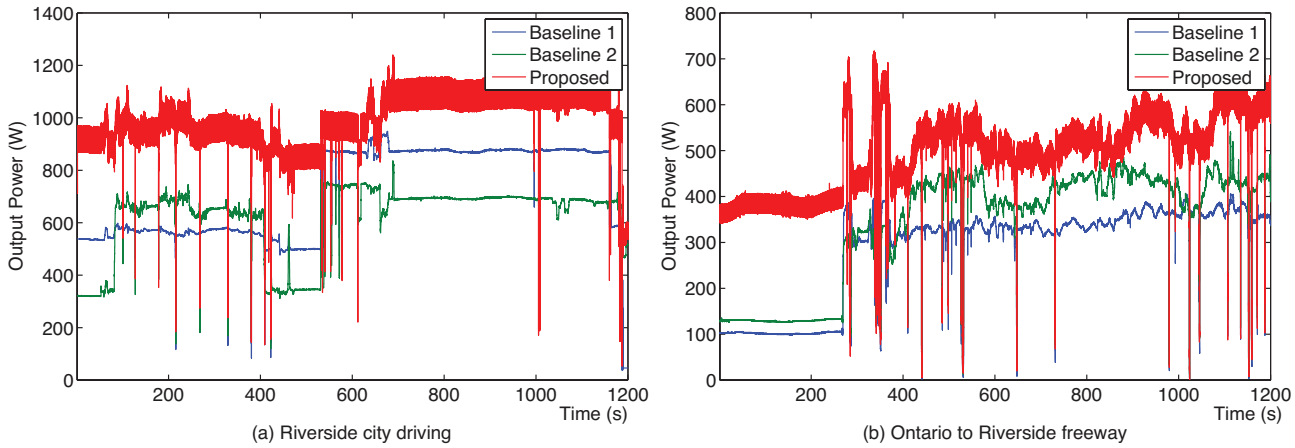

Figure 6: Performance comparison between the proposed reconfigurable PV system with baseline systems.

Table 4: Performance comparison between the optimal reconfigurable PV system with two customized PV systems on six benchmark profiles.

Benchmark	Optimal	Left Equip.	Right Equip.
Incheon Airport	1048W	945.3W	978.7W
Ontario to Riverside	518.5W	453.5W	429.9W
West LA to Indio	836.2W	770.7W	775.1W
West LA to Carson	785.7W	674.6W	715.9W
Riverside	1028W	969.9W	899.5W
West LA to Riverside	472.8W	403.3W	420.2W

side", partial PV installation will result in significant output power degradation. However, this is opposite for some other benchmark profiles such as “Riverside" or “Incheon Airport", because the solar irradiance levels on either the left side or right side (or both) of the vehicle is relatively low in the whole benchmark. In this cases, customized PV installation will be beneficial because it can significantly reduce the capital cost of the vehicular PV system. For example, if a user commutes through “Riverside" trace everyday such as a bus in a public transportation system, the customized PV installation reduces 22.3 % PV cell cost showing only 5.6 % reduction of power generation output.

7. CONCLUSIONS

In this paper, we propose fast online PV array reconfiguration and customization of the PV panel installation according to the driving pattern, in order to maximize the solar power generation for EVs. We implement a high-speed, high-voltage PV reconfiguration switch network with IGBTs and a reconfiguration controller. We derive the break-even time for reconfiguration and the corresponding adaptive reconfiguration policy based on solar irradiance/driving profiles using adaptive learning method, in which the on/off delay of IGBT, CAN delay, computation overhead, and energy overhead are taken into account. We also solve the design-time optimization problem of deriving the optimal size of each PV cell to achieve a desirable tradeoff of performance and reconfiguration complexity/overhead.

Acknowledgments

This research is supported by the Mid-Career Researcher Program and the International Research & Development Program of the NRF of Korea funded by the MSIP (NRF-2014-023320) and a grant from the Software and Hardware Foundations of the National Science Foundation.

8. REFERENCES

[1] D. Patterson and R. Spee, “The design and development of an axial flux permanent magnet brushless dc motor for wheel drive in a solar powered vehicle,” *IEEE Trans. Industry Applications*, vol. 31, no. 5, 1995.

[2] I. Arsie, G. Rizzo, and M. Sorrentino, “Optimal design and dynamic simulation of a hybrid solar vehicle,” *SAE Transactions-Journal of Engines*, 2007.

[3] *Solar powered vehicles: http://www.designboom.com/contemporary/solarpoweredvehicles.html*.

[4] A. Affanni, A. Bellini, G. Franceschini, P. Guglielmi, and C. Tassoni, “Battery choice and management for new-generation electric vehicles,” *IEEE Trans. Industrial Electronics*, 2005.

[5] W. Xiao, N. Ozog, and W. G. Dunford, “Topology study of photovoltaic interface for maximum power point tracking,” *IEEE Trans. Industrial Electronics*, 2007.

[6] X. Lin, Y. Wang, S. Yue, D. Shin, N. Chang, and M. Pedram, “Near-optimal dynamic module reconfiguration in a photovoltaic system to combat partial shading effects,” in *Proceedings of Design Automation Conference (DAC)*, June 2012.

[7] Y. Wang, X. Lin, N. Chang, and M. Pedram, “Dynamic reconfiguration of photovoltaic energy harvesting system in hybrid electric vehicles,” in *Proceedings of the International Symposium on Low Power Electronics and Design (ISLPED)*, Aug. 2012.

[8] Y. Wang, X. Lin, J. Kim, N. Chang, and M. Pedram, “Capital cost-aware design and partial shading-aware architecture optimization of a reconfigurable photovltaic system,” in *Proceedings of Design, Automation & Test in Europe (DATE)*, March 2013.

[9] C. M. Bishop, *Pattern Recognition and Machine Learning*. Springer, 2007.

[10] N. Femia, G. Petrone, G. Spagnuolo, and M. Vitelli, “Optimization of perturb and observe maximum power point tracking method,” *IEEE Trans. Power Electronics*, 2005.

[11] F. Liu, S. Duan, F. Liu, B. Liu, and Y. Kang, “A variable step size inc mppt method for pv systems,” *IEEE Trans. Industrial Electronics*, 2008.

[12] Y. Kim, N. Chang, Y. Wang, and M. Pedram, “Maximum power transfer tracking for a photovoltaic-supercapacitor energy system,” in *Proceedings of the International Symposium on Low Power Electronics and Design (ISLPED)*, Aug. 2010.

[13] Y. Wang, Y. Kim, Q. Xie, N. Chang, and M. Pedram, “Charge migration efficiency optimization in hybrid electrical energy storage (hees) systems,” in *Proceedings of the International Symposium on Low Power Electronics and Design (ISLPED)*, Aug. 2011.

[14] *Samsung Exynos 4 Dual 45nm (Exynos 4210) Microprocessor, 2012*.

[15] C. Hwang and C. Wu, “A predictive system shutdown method for energy saving of event-driven computation,” *ACM Trans. on Des. Autom. Electron. Systems*, 2000.